JOURNAL OF MATERIALS SCIENCE **34** (1999) 3597–3604

# Influence of $Y_2O_3$ distribution on the rate of tetragonal to monoclinic phase transformation of yttria-stabilized zirconia during hydrothermal aging

K. YASUDA, S. ARAI
*Materials and Devices Research Laboratories, Research and Development Center, Toshiba Corporation, Kawasaki 210, Japan*

M. ITOH, K. WADA
*Power and Industrial Systems Research and Development Center, Toshiba Corporation, Yokohama 235, Japan*
*E-mail: kazuhiro-yasuda@mdl.rdc.toshiba.co.jp*

Tetragonal to monoclinic phase transformation of yttria-stabilized zirconia, namely plasma-sprayed coatings and sintered bodies containing 4–8 mass % $Y_2O_3$ during hydrothermal aging was investigated with respect to $Y_2O_3$ distribution using 1 $\mu$m$\phi$ area from electron probe microanalysis (EPMA) and 20 nm$\phi$ area from transmission electron microscopy (TEM) analysis. Phase transformation at 473 K was prevented only in plasma-sprayed coatings having more than 6.7 mass % $Y_2O_3$ in 20 nm$\phi$ microscopic area. Furthermore, it was confirmed influence of $Y_2O_3$ distribution on the rate constants of this phase transformation was observed at 368 K. 

## 1. Introduction

Zirconia ceramics have excellent mechanical properties such as high fracture strength and high fracture toughness. They also have a high thermal expansion coefficient and low thermal conductivity. Therefore, plasma-sprayed stabilized zirconia, such as yttria-zirconia, has been developed for use as thermal barrier coatings (TBCs) for gas turbines and other engine components [1, 2].

In zirconia ceramics, however, degradation of mechanical properties occurs during low temperature aging because of tetragonal to monoclinic phase transformation [3–15]. Furthermore, it is reported that $Y_2O_3$ concentration, grain size, and stress affect the extent of tetragonal to monoclinic phase transformation in a humid atmosphere [4–8, 11–13, 16, 17].

Schubert *et al*. suggested that both $Y_2O_3$ distribution and grain size have to be carefully adjusted to suppress this degradation and that the critical $Y_2O_3$ concentration is between 4 and 5 mass % for 0.3 $\mu$m average grain size in sintered bodies for 573 K aging [13]. Yashima *et al*. suggested that 10 mol % $YO_{1.5}$-$ZrO_2$ arc-melt samples which had a homogeneous $Y_2O_3$ distribution underwent no transformation in hot water at 473 K, 200 MPa [15]. Previously, we studied plasma-sprayed, 8 mass % yttria-stabilized zirconia coatings which had a relatively uniform $Y_2O_3$ distribution ranging from 6.82 to 9.90 mass % according to EPMA analyses, and confirmed that the critical $Y_2O_3$ concentration to prevent the phase transformation was 6.3–6.8 mass % [18]. However, the EPMA probe diameter of 1 $\mu$m used in the above experiment was so large compared with the grain size of plasma-sprayed zirconia coating that its resolution was insufficient to analyze either $Y_2O_3$ distribution or critical concentration [19]. For this reason, observation of $Y_2O_3$ distribution in a more microscopic area is necessary to confirm the critical concentration precisely.

On the other hand, Yashima *et al*. also suggested that in zirconia ceramics containing high yttria concentration, the rate of tetragonal to monoclinic phase transformation decreases with increase of yttria concentration, and predicted that the rate of this phase transformation is affected by homogeneity of yttria concentration [15]. However, the relationship between the rate of this phase transformation and yttria distribution of yttria-stabilized zirconia was not obvious, because only limited quantitative data showing $Y_2O_3$ distribution were used in rate determination experiments of this phase transformation although the importance of $Y_2O_3$ distribution was reported. For this reason, the relationship between $Y_2O_3$ distribution and the rate of tetragonal to monoclinic phase transformation during hydrothermal aging has not been sufficiently confirmed. Furthermore, from the observation of tetragonal to monoclinic phase transformation in the 4–8 mass % $Y_2O_3$-$ZrO_2$ system at 473 K, $P_{H_2O} = 1.57$ MPa, it is difficult to prove the dependence of the rate on $Y_2O_3$ distribution, because phase transformation occurs rather rapidly in this test condition [18]. Hence, in order to clarify the

0022–2461  

relationship between $Y_2O_3$ concentration and the rate of transformation in a humid atmosphere with regard to $Y_2O_3$ distribution, aging experiments at lower temperatures than 473 K are desirable.

In this paper, we discuss the relationship between $Y_2O_3$ distribution and monoclinic phase fraction after hydrothermal aging at 473 K, $P_{H_2O} = 1.57$ MPa using a higher resolution TEM probe together with an EPMA probe to estimate critical $Y_2O_3$ concentration precisely. Furthermore, we investigated the rate of tetragonal to monoclinic phase transformation at both 368 K, $P_{H_2O} = 0.082$ MPa and 473 K, $P_{H_2O} = 1.57$ MPa to clarify the influence of both $Y_2O_3$ concentration and its distribution on the rate of transformation.

## 2. Experimental

Plasma-sprayed coatings and sintered bodies of yttria-stabilized zirconia used in this experiment had the following starting compositions: plasma-sprayed coatings: 4 mass % $Y_2O_3$-$ZrO_2$ (4YZ), 6 mass % $Y_2O_3$-$ZrO_2$ (6YZ), 8 mass % $Y_2O_3$-$ZrO_2$ (8YZA) and 8 mass % $Y_2O_3$-$ZrO_2$ (8YZB); sintered bodies: 2.5 mol % (4.5 mass %) $Y_2O_3$-$ZrO_2$ (25MYZ), 3.0 mol % (5.4 mass %) $Y_2O_3$-$ZrO_2$ (30MYZ) and 4.0 mol % (7.1 mass %) $Y_2O_3$-$ZrO_2$ (40MYZ).

The test piece of the plasma-sprayed coatings was composed of a substrate (SUS304; $70 \times 50 \times 3$ mm), a metal (NiCoCrAlY; Ni-23.8Co-16.7Cr-13.0Al-0.65Y; mass %) bonding layer and a $Y_2O_3$ stabilized zirconia layer. Thicknesses of the metal bonding layer and zirconia layer were 150 and 250 $\mu$m, respectively. The two layers were prepared by the atmospheric plasma-spray (APS) method under the conditions shown in Table I. 4YZ, 6YZ, and 8YZB layers were formed from fused and crushed powder and 8YZA layer was formed from agglomerated and sintered powder. Sintered bodies were obtained from a commercial source. All specimens were cut out of the plate and had dimensions of $10 \times 10 \times 3$ mm.

Average composition of the plasma-sprayed coatings and sintered bodies was determined by inductively coupled plasma (ICP) emission spectroscopy.

$Y_2O_3$ distribution of each zirconia coating and sintered body was measured by EPMA using a 3.0 mol % (5.4 mass %) $Y_2O_3$-$ZrO_2$ sintered body as the standard. On one specimen, 40 analysis points were selected, each point being 1 $\mu$m in diameter.

Both grain size and $Y_2O_3$ distribution for each zirconia coating and sintered body, namely the 4YZ, 6YZ, 8YZB, 25MYZ, 30MYZ and 40MYZ, were measured by TEM-EDX. On one specimen, more than 20 analysis points were selected, each point being 20 nm in diameter.

Hydrothermal aging tests were carried out using an autoclave in steam saturated air at pressures of 0.002–1.57 MPa, from room temperature to 473 K for 50 h, and at 368 K, $P_{H_2O} = 0.082$ MPa, for 0–1000 h.

Crystalline phases of the plasma sprayed surface layer were identified by X-ray diffraction (XRD) analysis. Scans of $2\theta$ between 27° and 33° were conducted to estimate the monoclinic to (tetragonal + cubic) zirconia ratio. The monoclinic fraction, $X_m$, is defined by the following equation [20]:

$$X_m = \frac{I(11\bar{1})_m + I(111)_m}{I(111)_m + I(111)_{t,c} + I(111)_m}.$$

where $I(11\bar{1})_m$ is the integrated intensity of the $(11\bar{1})$ reflection of the monoclinic phase, $I(111)_m$ is that of the (111) reflection of the monoclinic phase, and $I(111)_{t,c}$ is that of the (111) reflection of the tetragonal or cubic phase.

The rate constant, $k$, of the transformation was evaluated using the following equation:

$$\frac{X_m(t) - X_m(0)}{X_m(\infty) - X_m(0)} = 1 - \exp(-k \cdot t),$$

where $t$ is aging time, $X_m(t)$ is monoclinic phase fraction after aging for $t$, and $X_m(\infty)$ is saturated monoclinic phase fraction at aging temperature.

## 3. Results and discussion

### 3.1. Phase fraction of plasma-sprayed coatings and sintered bodies

Fig. 1a shows X-ray diffraction patterns of plasma-sprayed zirconia coatings. Plasma-sprayed coatings formed from fused and crushed powder, namely 4YZ, 6YZ and 8YZB, were composed almost exclusively of tetragonal zirconia, the fraction of monoclinic phase being negligible. However, 8YZA formed from agglomerated and sintered powder was a mixture of tetragonal phase and a small amount of monoclinic phase.

On the other hand, all sintered bodies were composed of tetragonal phase and a small amount of monoclinic phase (Fig. 1b).

Table II shows chemical composition of plasma-sprayed coatings and sintered bodies measured by ICP. The $Y_2O_3$ concentrations of both plasma-sprayed coatings and sintered bodies coincided with the starting composition. The samples can be lined up as follows in the order of increasing yttria concentration: 4YZ, 25MYZ, 30MYZ, 6YZ, 40MYZ, 8YZB and 8YZA.

TABLE I Plasma spraying parameters

| Parameter | | Value |
|---|---|---|
| Arc current | | 900 A |
| Arc voltage | | 37 V |
| Gas pressure | Ar | 0.34 MPa |
| | He | 0.34 MPa |
| Spray distance | | 8–11 $\times 10^{-2}$ m |

TABLE II $Y_2O_3$ composition in plasma-sprayed coatings and sintered bodies measured by ICP

| Samples | 4YZ | 6YZ | 8YZA | 8YZB | 25MYZ | 30MYZ | 40MYZ |
|---|---|---|---|---|---|---|---|
| $Y_2O_3$ (mass %) | 4.3 | 6.4 | 8.4 | 8.3 | 4.7 | 5.4 | 7.3 |

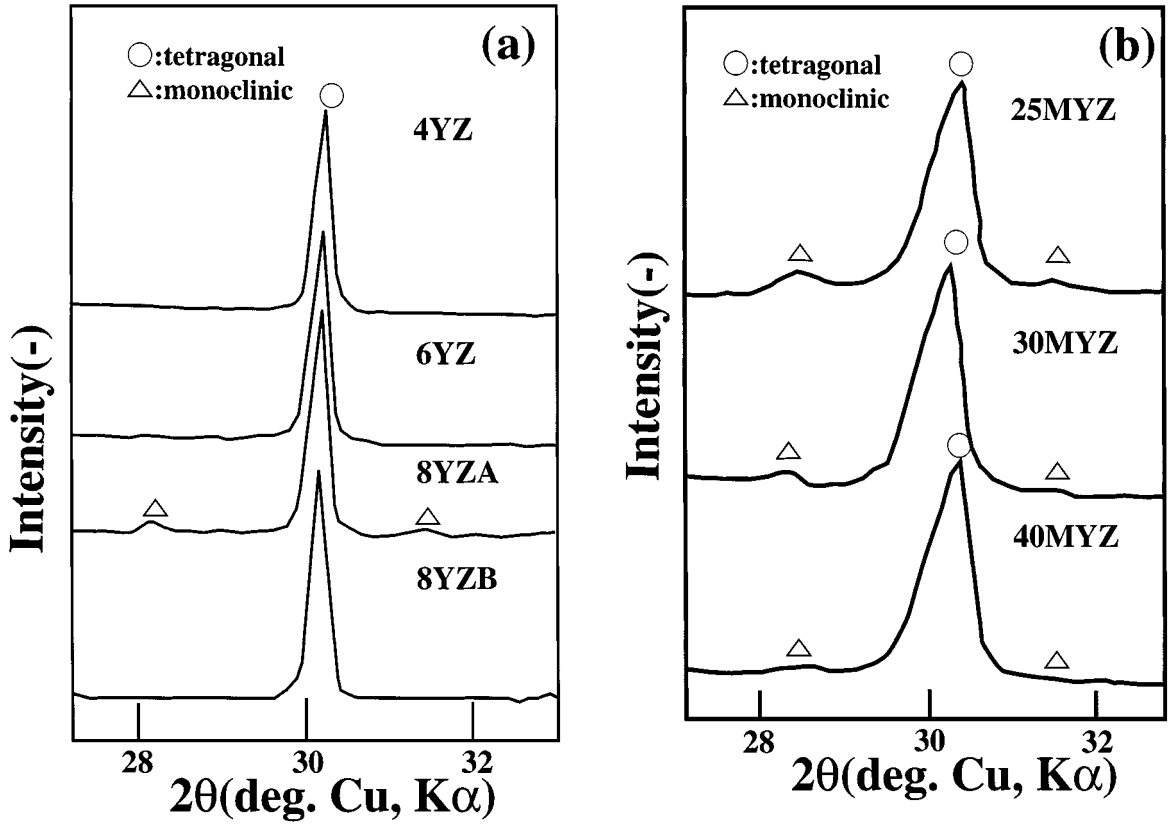


*Figure 1* X-ray diffraction patterns of (a) plasma-sprayed coatings and (b) sintered bodies.

### 3.2. $Y_2O_3$ distribution and grain size distribution

Table III shows $Y_2O_3$ distributions of both plasma-sprayed coatings and sintered bodies measured by both EPMA and TEM-EDX. As previously mentioned, plasma-sprayed coatings formed from fused and crushed powders, namely 4YZ, 6YZ and 8YZB, had relatively homogeneous $Y_2O_3$ distributions [18]. Standard deviation values were not larger than 0.6 mass %. In plasma-sprayed coatings formed from agglomerated and sintered powders, namely 8YZA, $Y_2O_3$ distribution was more heterogeneous than in 8YZB, and the range of $Y_2O_3$ distribution was from 1.33 to 14.82 mass %. Standard deviation was 2.50 mass %.

In contrast, standard deviations of $Y_2O_3$ distributions of sintered bodies 25MYZ, 30MYZ and 40MYZ were found to be smaller than 0.3 mass %. Homogeneity of $Y_2O_3$ distributions of sintered bodies 25MYZ, 30MYZ and 40MYZ was sharper than that of the plasma-sprayed coatings.

From the above results of EPMA analyses, it was clarified that $Y_2O_3$ distributions of both plasma-sprayed coatings 4YZ, 6YZ and 8YZB, but not 8YZA, and sintered bodies 25MYZ, 30MYZ and 40MYZ were relatively uniform. To be exact, $Y_2O_3$ distributions of sintered bodies were more uniform than those of plasma-sprayed coatings.

By comparison with the results of EPMA analysis, it was noticed that $Y_2O_3$ distributions of plasma-sprayed coatings measured by TEM were a little broader than those measured by EPMA. However, the range of $Y_2O_3$ distribution for each plasma-sprayed coating from TEM observation approximately coincided with that from EPMA observation. In particular, minimum $Y_2O_3$ concentrations observed by both analyses were very similar, except for 4YZ. However, minimum $Y_2O_3$ concentration of 4YZ from TEM observation was not less than that from EPMA observation.

On the other hand, $Y_2O_3$ distributions of sintered bodies measured by TEM were also broader than those measured by EPMA. However, the minimum $Y_2O_3$

TABLE III $Y_2O_3$ distribution of both plasma-sprayed coatings and sintered bodies measured by both EPMA and TEM

| | Minimum (mass %) | | Maximum (mass %) | | Mean (mass %) | | Standard deviation | |
|---|---|---|---|---|---|---|---|---|
| Sample | EPMA | TEM | EPMA | TEM | EPMA | TEM | EPMA | TEM |
| 4YZ | 2.39 | 4.26 | 5.81 | 8.08 | 4.59 | 5.92 | 0.57 | 0.83 |
| 6YZ | 5.27 | 5.42 | 7.50 | 8.24 | 6.77 | 6.72 | 0.40 | 0.88 |
| 8YZA | 1.33 | — | 14.82 | — | 7.96 | — | 2.50 | — |
| 8YZB | 6.82 | 6.79 | 9.90 | 12.53 | 7.57 | 9.88 | 0.61 | 1.22 |
| 25MYZ | 4.30 | 4.29 | 5.19 | 6.43 | 4.65 | 5.24 | 0.18 | 0.52 |
| 30MYZ | 5.11 | 4.92 | 5.80 | 8.07 | 5.37 | 6.20 | 0.16 | 0.78 |
| 40MYZ | 6.78 | 3.83 | 7.37 | 8.45 | 7.25 | 6.15 | 0.29 | 1.23 |

concentrations observed by the two analyses in both 25MYZ and 30MYZ were identical. Whereas, compared with EPMA analysis, the range of $Y_2O_3$ distribution in 40MYZ measured by TEM was much broader, extending to much lower $Y_2O_3$ concentration than 6.78 mass %, which was the minimum $Y_2O_3$ concentration observed by EPMA analyses.

To summarize the results shown in Table III, $Y_2O_3$ distributions in 4YZ, 6YZ, 8YZB, 25MYZ and 30MYZ from EPMA analyses (1 $\mu$m$\phi$) coincided with those in the more microscopic range (20 nm$\phi$). On the other hand, $Y_2O_3$ distributions in the sintered body 40MYZ obtained by EPMA analyses (1 $\mu$m$\phi$) were inconsistent with those obtained by TEM. From these results, it was found that $Y_2O_3$ distributions of 4YZ, 6YZ, 8YZB, 25MYZ and 30MYZ were relatively uniform even in the TEM observation area, 20 nm$\phi$. However, $Y_2O_3$ distributions of 40MYZ were not uniform in the same area.

The range of grain size of all samples was from 0.04 to 0.73 $\mu$m as shown in Table IV. The grain size was much smaller than the EPMA probe diameter, although greater than the TEM probe diameter. Mean grain size ranged from 0.17 to 0.24 $\mu$m and more than 80% of grains of each sample ranged from 0.05 to 0.3 $\mu$m. Furthermore, no clear relationship was observed between grain size and $Y_2O_3$ concentration.

TABLE IV Grain size distribution of both plasma-sprayed coatings and sintered bodies measured by TEM

| Sample | Minimum | Maximum | Mean | Standard deviation |
|---|---|---|---|---|
| 4YZ | 0.09 $\mu$m | 0.73 $\mu$m | 0.24 $\mu$m | 0.12 $\mu$m |
| 6YZ | 0.08 | 0.33 | 0.15 | 0.04 |
| 8YZB | 0.08 | 0.42 | 0.19 | 0.09 |
| 25MYZ | 0.04 | 0.43 | 0.19 | 0.09 |
| 30MYZ | 0.04 | 0.55 | 0.18 | 0.10 |
| 40MYZ | 0.08 | 0.51 | 0.18 | 0.08 |

## 3.3. Phase transformation after hydrothermal aging

Fig. 2 shows temperature dependence of monoclinic phase fraction of coatings and sintered bodies after aging test for 50 h. Increment of monoclinic phase was observed in 4YZ, 6YZ, 8YZA, 25MYZ, 30MYZ and 40MYZ. Only in 8YZB was increment not observed.

Fig. 3 shows monoclinic phase fraction after aging at 473 K for 0–100 h. In all samples the fraction saturated after aging for 10 h. Monoclinic phase fraction after aging at 473 K decreased for each sample with $Y_2O_3$ concentration.

Comparing 40MYZ and 8YZB, $Y_2O_3$ distributions measured by EPMA shown in Table III were found to be almost consistent and minimum concentration of $Y_2O_3$ was 6.78 and 6.82 mass %, respectively. However, $Y_2O_3$ distribution of these samples measured by TEM-EDX ranged from 3.83 to 8.45 and from 6.79 to 12.53, respectively. From these results, it is suggested that in 40MYZ the phase transformation occurred selectively in the grains which had lower $Y_2O_3$ concentration.

In summary, it is concluded that tetragonal to monoclinic phase transformation during hydrothermal aging did not occur in tetragonal zirconia which had more than 6.7 mass % $Y_2O_3$ in the microscopic (20 nm$\phi$) area as well as in the 1 $\mu$m$\phi$ area.

Fig. 4 shows time dependence of monoclinic phase fraction of coatings after aging test at 368 K, $P_{H_2O} = 0.082$ MPa. The test time was varied from 0 to 1000 h. In 8YZB, transformation did not occur at 368 K after 1000 h.

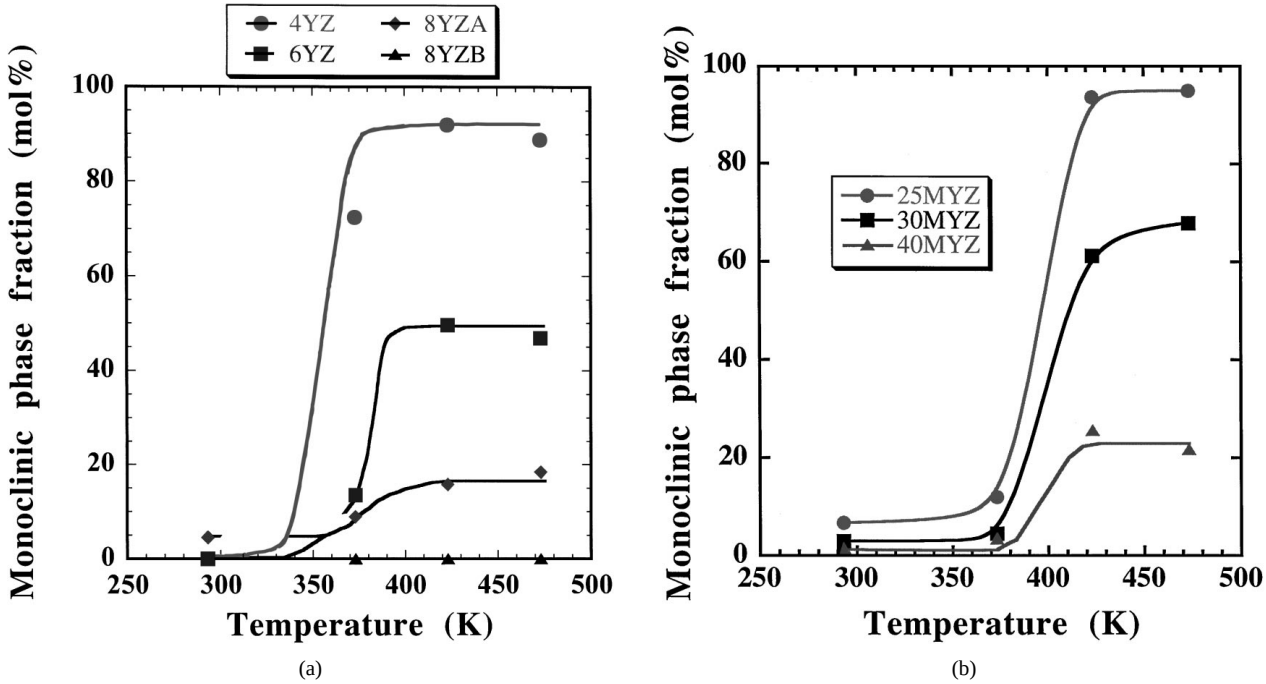


*Figure 2* Monoclinic phase fraction of plasma-sprayed coatings and sintered bodies having different yttria content after aging in saturated steam atmosphere at 293, 343, 368, 373, 423 and 473 K. (a) Plasma-sprayed coatings and (b) sintered bodies.

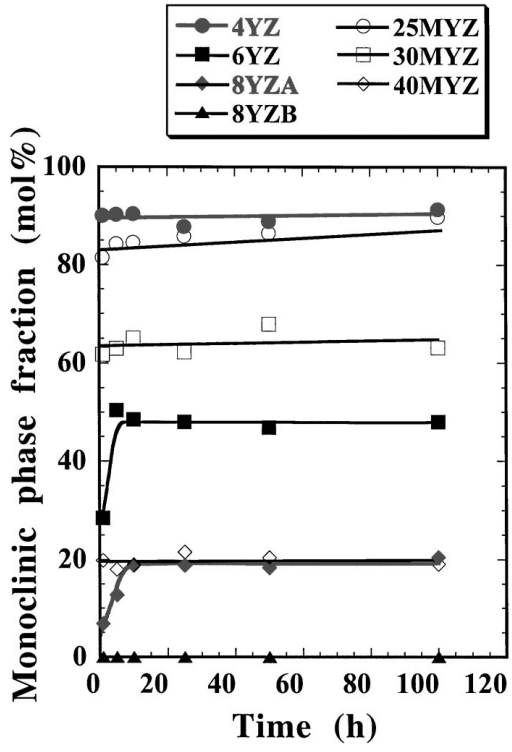


*Figure 3* Monoclinic phase fraction after aging at 473 K, $P_{H_2O} =$ 1.57 MPa for 0–100 h.

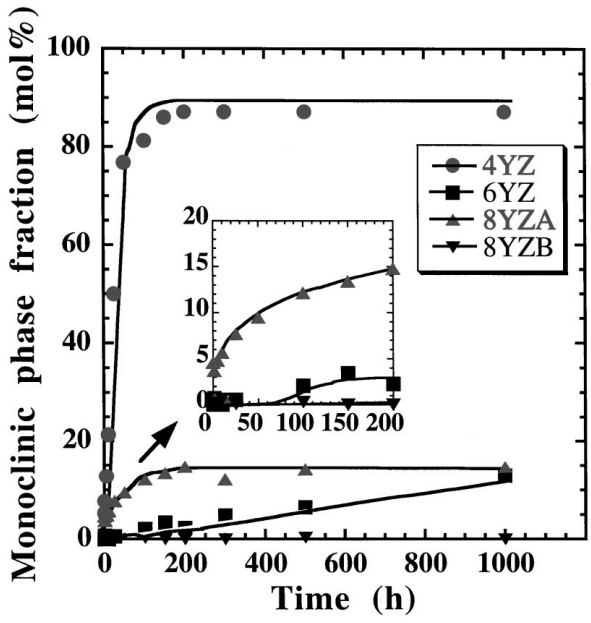


*Figure 4* Monoclinic phase fraction of plasma-sprayed coatings after aging at 368 K, $P_{H_2O} = 0.082$ MPa for 0–1000 h.

In both 4YZ and 8YZA, increase of monoclinic phase was observed within 100 h. In particular, monoclinic phase fraction of 8YZA after 100 h reached more than 66% of $X_m(\infty)_{368\ K}$. Furthermore, within 200 h, the monoclinic phase fraction saturated in both 4YZ and 8YZA.

On the other hand, in 6YZ, tetragonal to monoclinic phase transformation was not observed within 100 h. However, the phase transformation started after 100 h. As shown in Fig. 3, after 473 K aging it was observed that the monoclinic phase fraction in 6YZ was always greater than that in 8YZA. However, the reversal of monoclinic phase fraction after 368 K aging within 1000 h was observed in 6YZ and 8YZA.

As shown in Fig. 4, it was observed that the start of phase transformation in 6YZ was delayed compared with those of 4YZ and 8YZA. As shown in Table III, $Y_2O_3$ distributions of 4YZ and 8YZA ranged from 2.39 to 5.81 mass % and from 1.33 to 14.82 mass %, respectively. While, 6YZ contained a negligible amount of tetragonal zirconia which had less than 5.27 mass % $Y_2O_3$. Fig. 5 shows the detail of $Y_2O_3$ distribution of 4YZ, 6YZ and 8YZA. Tetragonal to monoclinic phase transformation occurred in zirconia which had less than

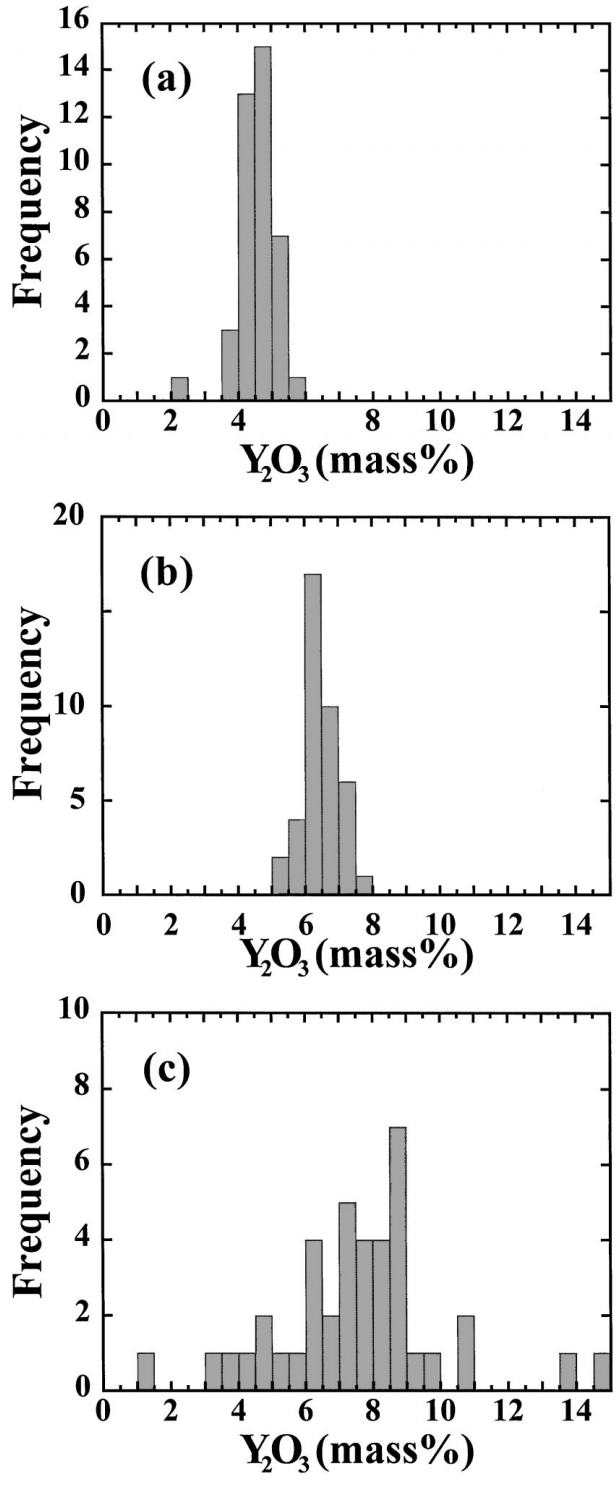


*Figure 5* Distribution of $Y_2O_3$ concentration in plasma-sprayed coatings measured by EPMA: (a) 4YZ, (b) 6YZ, and (c) 8YZA.

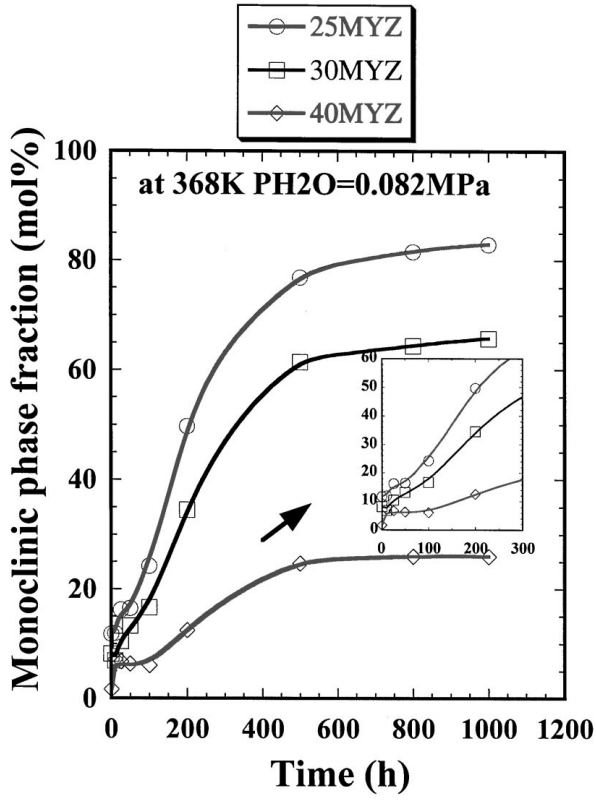


*Figure 6* Monoclinic phase fraction of sintered bodies after aging at 368 K, $P_{H_2O} = 0.082$ MPa.

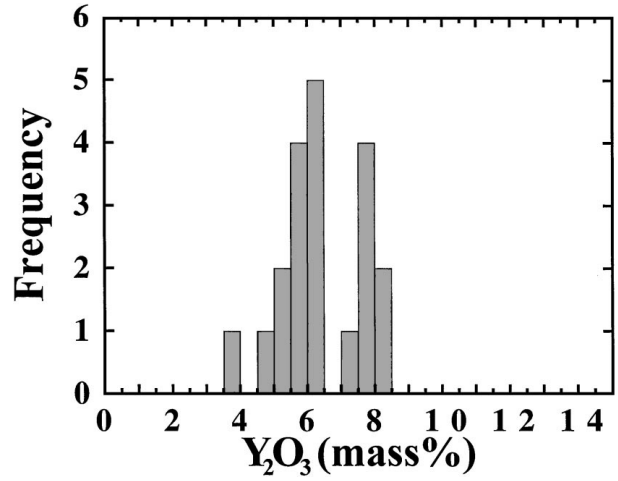


*Figure 7* Distribution of $Y_2O_3$ concentration in 40MYZ measured by TEM-EDX.

6.3–6.8 mass % $Y_2O_3$ even at 473 K [18]. For that reason, monoclinic phase fraction after aging could almost be estimated based on the proportion of tetragonal zirconia which contains less than 6.5 mass % $Y_2O_3$, using Fig. 5. 8YZA had a smaller area containing less than 6.5 mass % $Y_2O_3$ than 6YZ. However, if the area was defined as that with less than 5 mass % $Y_2O_3$, the area in 8YZA was greater than that in 6YZ. From these results, it was suggested that in hydrothermal aging at 368 K, $P_{H_2O} = 0.082$ MPa, until 100 h, tetragonal to monoclinic phase transformation occurred in the region containing less $Y_2O_3$ than 5 mass % in 4YZ and 8YZA and that after 100 h phase transformation started in the region containing more $Y_2O_3$ than 5 mass %, As a result, phase transformation in the 6YZ seems to start after 100 h.

Fig. 6 shows time dependence of monoclinic phase fraction of the sintered bodies after aging test at 368 K, $P_{H_2O} = 0.082$ MPa. The aging test time was varied between 0 and 1000 h. Increase of monoclinic phase was observed in all sintered bodies and monoclinic phase fractions saturated within 800 h.

However, a unique transformation behavior was observed in 40MYZ. The monoclinic phase fraction saturated temporarily within 10 h. That value was maintained until 100 h. Then, the monoclinic fraction started to increase again and saturated in 500 h. Fig. 7 shows the $Y_2O_3$ distribution of 40MYZ from TEM-EDX observation. As shown in Fig. 7, $Y_2O_3$ distribution of 40MYZ ranged from 3.83 to 8.45 mass %, and in the greater part of the specimen $Y_2O_3$ concentration was larger than 5 mass %. It is suggested that in 40MYZ, until 100 h, tetragonal to monoclinic phase transformation occurred in the region having less than 5 mass % $Y_2O_3$, and that after 100 h the phase transformation started in the region having more than 5 mass % $Y_2O_3$.

From these results, we suggest that the tetragonal to monoclinic phase transformation at 368 K, $P_{H_2O} = 0.082$ MPa progresses as follows.

1. Until 100 h, tetragonal zirconia which contains less than 5 mass % $Y_2O_3$ transforms to monoclinic phase rapidly.
2. After 100 h, tetragonal zirconia whose $Y_2O_3$ concentration lies between 5 mass % and critical $Y_2O_3$ concentration transforms to monoclinic phase slowly.

In the case that temperature and $H_2O$ pressure were raised, it is suggested that the phase transformation was accelerated and the difference between step 1 and step 2 disappeared. For that reason, the multistage reaction in this phase transformation was not observed at 473 K.

## 3.4. Rate of phase transformation

### *3.4.1. Plasma-sprayed coatings*

Figs 8 and 9 show rate constant of transformation of plasma-sprayed coatings and sintered bodies at 368 and 473 K. In plasma-sprayed coatings, the rate decreased with an increase of $Y_2O_3$ concentrations in zirconia which had homogeneous $Y_2O_3$ distributions. Rate constants at 368 K were less than 1/100 of those at 473 K.

At 368 K rate constant of 6YZ was lower than that of 8YZA which had heterogeneous $Y_2O_3$ distribution, whereas at 473 K the rate constant of 6YZ was greater than that of 8YZA. Comparing rate constants of 6YZ and 8YZA in the experiment at both 368 and 473 K, it is suggested that homogeneity of $Y_2O_3$ distribution influenced the rate constant of tetragonal to monoclinic phase transformation at 368 K.

The $Y_2O_3$ concentration dependence on the rate constant almost agreed with the results of Yashima *et al.* [15]. However, their values of the rate constant at low $Y_2O_3$ concentration disagreed with those in the present work, due to the different test conditions (form and phase composition of starting sample, experimental atmosphere, etc.). In particular, they used zirconia

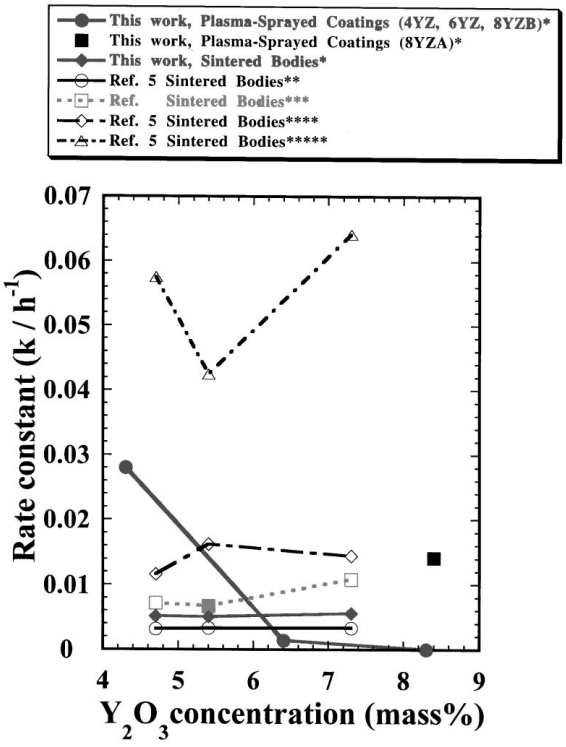


*Figure 8* Relationship between rate constant of transformation of plasma-sprayed coatings and sintered bodies. *: at 368 K, $P_{H_2O} =$ 0.082 MPa, **: at 356 K in water, ***: at 368 K in water, ****: at 378 K in water.

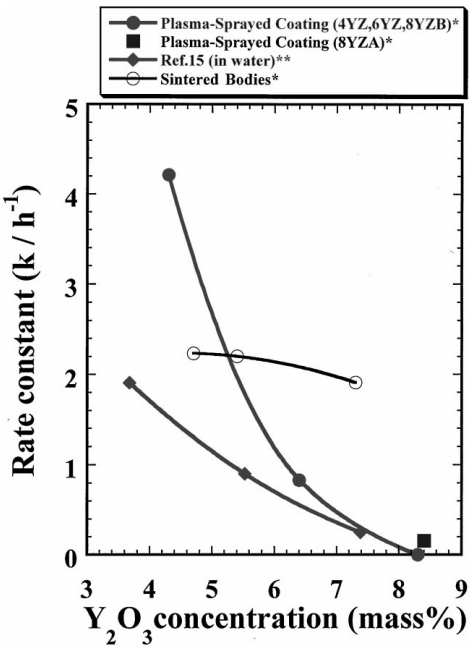


*Figure 9* Relationship between rate of transformation of plasma-sprayed coatings and sintered bodies. *: at 473 K, $P_{H_2O} = 1.57$ MPa, **: at 473 K, 200 MPa.

powders which were composed of a large quantity of monoclinic phase as starting samples. For that reason, it is thought that fraction of monoclinic phase which was formed by phase transformation after aging decreased and the measured rate of transformation was lower.

### 3.4.2. Sintered bodies

In sintered bodies, the $Y_2O_3$ concentration dependence on rate constants of transformation at both 368 and 473 K was not observed. Furthermore, comparing plasma-sprayed coatings and sintered bodies, rate constants of sintered bodies which had lower than 5–6 mass % $Y_2O_3$ concentration were lower than those of plasma-sprayed coatings. Conversely, rate constant in a sintered body which had higher than 5–6 mass % $Y_2O_3$ concentration was greater than that of plasma-sprayed coating. These results seem to originate from the following facts.

1. Porosity of sintered bodies was much less than that of coatings [21]. Tetragonal to monoclinic phase transformation under hydrothermal aging occurred from the surface [7]. In both 25MYZ and 30MYZ, it was suggested that sufficient transformation did not occur in a short time because of steam supply shortage.
2. The $Y_2O_3$ distribution in 40MYZ was not uniform. Some areas of 40MYZ contain less $Y_2O_3$ than the critical concentration, as revealed by TEM-EDX observation and shown in both Table III and Fig. 7. As a result, it is suggested that phase transformation in the 40MYZ occurred in the limited areas containing less $Y_2O_3$.

Tetragonal to monoclinic phase transformation which occurs in a humid atmosphere at low temperatures was influenced by residual stress besides $Y_2O_3$ concentration and grain size [4–8, 11–13, 16, 17]. In order to investigate both critical $Y_2O_3$ concentration and relationship between rate of the phase transformation and $Y_2O_3$ concentration, the influence of stress on this transformation must be clarified.

## 4. Conclusion

In this paper, tetragonal to monoclinic phase transformation in plasma-sprayed coatings and sintered bodies in the $Y_2O_3$-$ZrO_2$ system has been investigated. Phase transformation selectively occurred in microscopic area containing less $Y_2O_3$ than 6.7 mass % at 473 K in a humid atmosphere. Furthermore, in tetragonal zirconia coatings which had relatively uniform $Y_2O_3$ distribution, the influence of $Y_2O_3$ distribution on the rate constant was observed at a lower temperature, 368 K. The most interesting point is that in both plasma-sprayed coatings and sintered bodies, multistage behavior which reflected the $Y_2O_3$ distribution in the microscopic areas was observed in the tetragonal to monoclinic phase transformation at 368 K aging.

## References

1. S. STECURA, *Amer. Ceram. Soc. Bull.* **56** (1977) 1082.
2. F. VASILIU and I. PENCEA, *ibid.* **64** (1985) 1268.
3. K. KOBAYASHI, H. KUWAJIMA and T. MASAKI, *Solid State Ionics* **3/4** (1981) 489.
4. T. SATO and M. SHIMADA, *J. Amer. Ceram. Soc.* **67** (1984) C-212.
5. *Idem., ibid.* **68** (1985) 356.
6. K. TSUKAMA and M. SHIMADA, *J. Mater. Sci. Lett.* **4** (1985) 857.
7. T. SATO, S. OHTAKI and M. SHIMADA, *J. Mater. Sci.* **20** (1985) 1466.
8. T. SATO and M. SHIMADA, *ibid.* **20** (1985) 3988.
9. T. SATO, S. OHTAKI, T. ENDO and M. SHIMADA, *J. Amer. Ceram. Soc.* **68** (1985) C320.

10. F. F. LANGE, G. L. DUNLOP and B. I. DAVIS, *ibid*. **69** (1986) 237.
11. T. SATO, H. FUJISHIRO, T. ENDO and M. SHIMADA, *J. Mater. Sci.* **22** (1987) 882.
12. T. SATO, S. OHTAKI, T. ENDO and M. SHIMADA, in "Advanced Ceramics," Vol. 24A, Science and Technology of Zirconia 3, edited by S. Somiya, N. Yamamoto and H. Yanagida (American Ceramics Society, Westerville, OH, 1988) p. 29.
13. H. SCHUBERT and G. PETZOW, *ibid*. p. 21.
14. M. HIRANO and H. INADA, *J. Mater. Sci*. **26** (1991) 5047.
15. M. YASHIMA, T. NAGATOME, T. NOMA, N. ISHIZAWA, Y. SUZUKI and M. YOSHIMURA, *J. Amer. Ceram. Soc*. **78** (1995) 2229.
16. A. J. A. WINNUBST and A. J. BURGGRAF, in "Advanced Ceramics," Vol. 24A, Science and Technology of Zirconia 3, edited by S. Somiya, N. Yamamoto and H. Yanagida (American Ceramics Society, Westerville, OH, 1988) p. 39.
17. F. F. LANGE, *J. Mater. Sci*. **17** (1982) 225.
18. K. YASUDA, M. ITOH, S. ARAI, T. SUZUKI and M. NAKAHASHI, *ibid*. **32** (1997) 6291.
19. P. D. HARMSWORTH and R. STEVENS, *ibid*. **27** (1992) 611.
20. R. C. GRAVIE and P. S. NICHOLSON, *J. Amer. Ceram. Soc*. **55** (1972) 303.
21. S. SAFAI and H. HERMAN, *Thin Solid Films* **45** (1977) 295.

*Received 22 September 1998*
*and accepted 11 February 1999*